SENSOR AND SIMULATION NOTES

Note 324

April 1990

THE EXTERNAL ENVIRONMENT OF VPD-II:

GROUND-WAVE FIELD

Kendall F. Casey

JAYCOR

39650 Liberty Street, Suite 320

Fremont, CA 94538

Abstract

The electromagnetic field of the VPD-II EMP environment simulator is considered, with particular attention being given to the field near the air-ground interface. The simulator antenna is modeled as a distribution of conical ring dipoles. The frequency-domain radiated field is evaluated asymptotically using saddle-point integration techniques. Time-domain results are obtained using numerical inverse Fourier transforms. It is found that, for typical pulser charge voltages, the field close to the air-ground interface is less than one kV/m at a range of one kilometer.

1 Introduction

In a previous note [1] we considered the electromagnetic field of the VPD-II EMP environment simulator, confining our attention to the far-zone space-wave contribution to the total field. This contribution vanishes as the observer position approaches the air-ground interface. To complete the description of the VPD-II field, one must also consider the ground-wave contribution. This contribution to the total field is dominant for observers near the interface. We consider the total field of VPD-II in this note, giving particular attention to the ground wave.

In the next section we consider the electromagnetic field of a conical ring dipole over an imperfect ground. This source, which is modeled by a closely spaced pair of magnetic-current loops, represents a ring-shaped segment of the VPD-II antenna. Then in Section 3 we carry out the asymptotic evaluation of the conical ring dipole field and obtain the space-wave and ground-wave contributions to this field. The integration over a distribution of conical ring dipoles is carried out in Section 4, wherein we evaluate the space-wave and ground-wave contributions to the field of the VPD-II antenna in the frequency domain. Numerical results for the time-domain electric field radiated by VPD-II are presented and discussed in Section 5. We use equivalent circuits which represent the Marx generator and the antenna input impedance to obtain the frequency-domain current at the antenna feed point. The time-domain radiated electromagnetic field is then obtained via numerical inverse Fourier transformation. Section 6 concludes the note.

2 Field of a Conical Ring Dipole Over an Imperfect Ground

The VPD-II antenna is a resistively loaded wire mesh cone. The resistive loading on the antenna is designed to produce a surface current density $\vec{J}_s(\vec{r}\,', t)$ which behaves as

$$\vec{J}_s(\vec{r}\,', t) = \frac{I_0(t - r'/c)(1 - r'/r_0)}{2\pi r' \sin\theta_0}\,\vec{a}_{r'} \qquad (0 \le r' \le r_0) \tag{1}$$

where r' is the radial coordinate along the surface of the cone and r_0 is the slant height. The unit vector in the radial direction on the cone, whose internal half-angle is θ_0, is $\vec{a}_{r'}$. The current at the feed point is $I_0(t)$ and c denotes the speed of light. Since the surface current density vanishes at $r' = r_0$, radiation from the upper edge of the antenna and from the top cap is small.

The surface current density on the antenna is given in the frequency domain (the time dependence $\exp(j\omega t)$ is assumed) by

$$\tilde{\vec{J}}_s(\vec{r}\,') = \frac{\tilde{I}_0(j\omega)(1 - r'/r_0)e^{-jkr'}}{2\pi r' \sin\theta_0}\,\vec{a}_{r'} \qquad (0 \le r' \le r_0) \tag{2}$$

where $\tilde{I}_0(j\omega)$ is the frequency-domain current at the base of the antenna and $k = \omega/c$ is the free-space propagation constant. We define a "conical ring dipole" as the segment of the antenna lying between r' and $r' + dr'$, for $\theta = \theta_0$. It is not difficult to show using duality [2] that the field radiated by this source is identical to that of two magnetic-current loops carrying equal and opposite magnetic currents $\pm V_0$ and located at $r = r'$, $\theta = \theta_0$ and $\theta_0 - d\theta_0$ with

magnetic currents $\pm V_0$ and located at $r = r'$, $\theta = \theta_0$ and $\theta_0 - d\theta_0$ with

$$V_0 d\theta_0 = -\frac{Z_0 \tilde{I}(r')dr'}{2\pi j k r'^2 \sin\theta_0} \tag{3}$$

where Z_0 denotes the intrinsic impedance of free space and

$$\tilde{I}(r') = \tilde{I}_0(j\omega)e^{-jkr'}(1 - r'/r_0) \qquad (0 \leq r' \leq r_0) \tag{4}$$

Integration over a set of such sources yields the field of the VPD-II antenna. We therefore begin by considering the field of a single magnetic-current loop over an imperfect ground.

2.1 Field of a Magnetic-Current Loop

The geometry of the problem is shown in Figure 1. A loop of magnetic current V_0 is centered on the z-axis at $z = z' > 0$. The radius of the loop is ρ' and the plane of the loop is parallel to the $z = 0$ plane. The region $z > 0$ is free space. The region $z < 0$ is an imperfectly conducting medium of (complex) relative permittivity $\hat{\epsilon}_r$.

The electromagnetic field is independent of the azimuthal coordinate ϕ by symmetry. Its components are $\tilde{E}_\rho, \tilde{E}_z$, and $\tilde{H}_\phi$, which can be expressed in terms of a scalar function ψ by

$$\tilde{E}_\rho = \frac{Z_0}{jkq}\frac{\partial^2\psi}{\partial\rho\partial z} \tag{5}$$

$$\tilde{E}_z = \frac{Z_0}{jkq}\left(k^2 q + \frac{\partial^2}{\partial z^2}\right)\psi \tag{6}$$

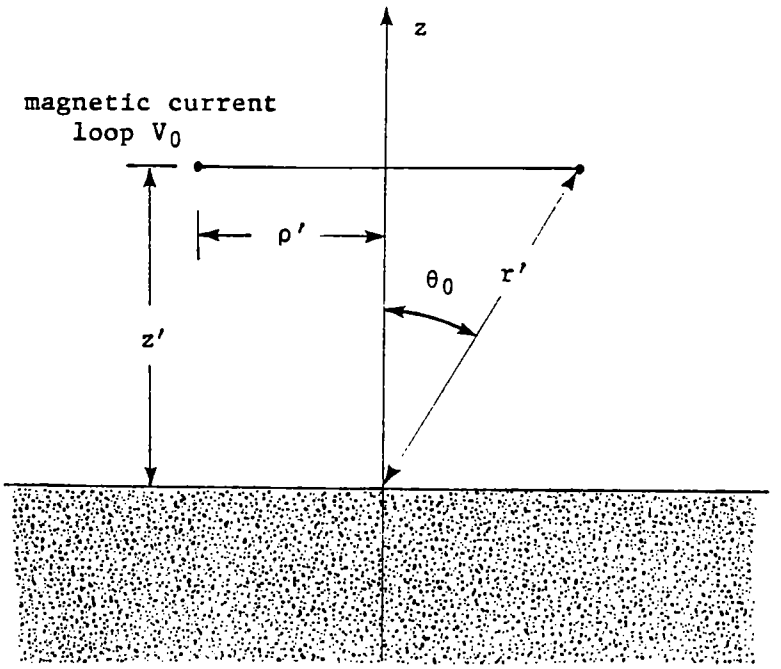

Figure 1: Geometry of the problem.

$$\tilde{H}_\phi = -\frac{\partial \psi}{\partial \rho} \tag{7}$$

The function ψ satisfies the scalar Helmholtz equation, subject to appropriate boundary conditions; and $q = 1$ for $z > 0$, $q = \hat{\epsilon}_r$ for $z < 0$. Expressions for ψ which are appropriate for the air and ground regions are

$$z > 0: \quad \psi_> = \int_0^\infty A_p(\lambda) J_0(\lambda\rho) e^{-j\sqrt{k^2-\lambda^2}\,|z-z'|} d\lambda \tag{8}$$

$$+ \int_0^\infty R(\lambda) A_p(\lambda) J_0(\lambda\rho) e^{-j\sqrt{k^2-\lambda^2}\,(z+z')} d\lambda$$

$$z < 0: \quad \psi_< = \int_0^\infty [1 + R(\lambda)] A_p(\lambda) J_0(\lambda\rho) e^{j\sqrt{k^2\hat{\epsilon}_r-\lambda^2}\,z} e^{-j\sqrt{k^2-\lambda^2}\,z'} d\lambda \tag{9}$$

where the function $A_p(\lambda)$ describes the field radiated by the magnetic-current loop in the absence of the ground. The function $R(\lambda)$ is to be determined and $J_0(\cdot)$

denotes the Bessel function of order zero. The square roots are to be taken such that $\Im\sqrt{k^2-\lambda^2} \leq 0$ and $\Im\sqrt{k^2\hat{\epsilon}_r-\lambda^2} \leq 0$ to ensure satisfaction of the radiation condition as $z \to \pm\infty$.

The expressions for ψ given in eqs. (8) and (9) above ensure that $\tilde{H}_\phi$ is continuous at $z = 0$. In order that $\tilde{E}_\rho$ be continuous at $z = 0$, it is necessary that

$$\sqrt{k^2\hat{\epsilon}_r-\lambda^2}\,[1+R(\lambda)] = \hat{\epsilon}_r\sqrt{k^2-\lambda^2}\,[1-R(\lambda)] \tag{10}$$

whence we obtain

$$R(\lambda) = \frac{\hat{\epsilon}_r\sqrt{k^2-\lambda^2}-\sqrt{k^2\hat{\epsilon}_r-\lambda^2}}{\hat{\epsilon}_r\sqrt{k^2-\lambda^2}+\sqrt{k^2\hat{\epsilon}_r-\lambda^2}} \tag{11}$$

The function $R(\lambda)$ is simply the Fresnel reflection coefficient for plane waves polarized parallel to the plane of incidence, expressed in terms of the spectral variable λ.

The primary-excitation function $A_p(\lambda)$ is found by enforcing the condition that

$$\tilde{E}_\rho(\rho, z'+) - \tilde{E}_\rho(\rho, z'-) = -V_0\delta(\rho-\rho') \tag{12}$$

Thus it is necessary that

$$\frac{2Z_0}{k}\int_0^\infty \sqrt{k^2-\lambda^2}\,A_p(\lambda)J_1(\lambda\rho)\lambda d\lambda = -V_0\delta(\rho-\rho') \tag{13}$$

whence we obtain, upon inversion of the Fourier-Bessel transform,

$$A_p(\lambda) = \frac{-kV_0\rho' J_1(\lambda\rho')}{2Z_0\sqrt{k^2-\lambda^2}} \tag{14}$$

which completes the solution for the field of the magnetic-current loop over an imperfect ground.

2.2 Field of a Conical Ring Dipole

Now write ρ' and z' in terms of the spherical source coordinates r' and θ_0 as

$$\rho' = r' \sin\theta_0 \tag{15}$$

$$z' = r' \cos\theta_0 \tag{16}$$

and construct the field of a second magnetic-current loop (carrying magnetic current $-V_0$) at $r', \theta_0 - d\theta_0$. The total potential $d\psi_t$ due to the two sources is given for $z > z'$ by

$$d\psi_t = \frac{-kr'V_0 d\theta_0}{2Z_0} \int_0^\infty J_0(\lambda\rho) \frac{d}{d\theta_0} F(r';\theta_0;\lambda)\, \frac{e^{-j\sqrt{k^2-\lambda^2}\,z} d\lambda}{\sqrt{k^2-\lambda^2}} \tag{17}$$

where

$$\begin{aligned} F(r';\theta_0;\lambda) &= \sin\theta_0 J_1(\lambda r' \sin\theta_0) \left[e^{j\sqrt{k^2-\lambda^2}\, r' \cos\theta_0} \right. \\ &+ \left. R(\lambda) e^{-j\sqrt{k^2-\lambda^2}\, r' \cos\theta_0} \right] \end{aligned} \tag{18}$$

Substituting for $V_0 d\theta_0$ from eq. (3), converting the integral in eq. (17) into one along the entire λ-axis, and using eq. (7), we obtain the magnetic field of the conical ring dipole over an imperfect ground in the region $z > z'$:

$$d\tilde{H}_\phi = \frac{\tilde{I}(r')dr'}{8\pi j r' \sin\theta_0} \int_{-\infty}^{\infty} H_1^{(2)}(\lambda\rho) e^{-j\sqrt{k^2-\lambda^2}\, z} \cdot \tag{19}$$

$$\frac{d}{d\theta_0} F(r';\theta_0;\lambda) \frac{\lambda d\lambda}{\sqrt{k^2-\lambda^2}}$$

where $H_1^{(2)}(\cdot)$ denotes the Hankel function of the second kind, of order one. We now consider the evaluation of this field when $k\sqrt{\rho^2+z^2} \to \infty$.

3 Asymptotic Evaluation of the Conical Ring Dipole Field

In this section we carry out the asymptotic evaluation of the field of the conical ring dipole over an imperfect ground. In so doing, we obtain the space-wave and the ground-wave contributions to the total field. We begin by introducing the large-argument asymptotic form for the Hankel function

$$H_1^{(2)}(x) \sim j\sqrt{\frac{2j}{\pi x}}\, e^{-jx} \quad (x \to \infty) \tag{20}$$

and making the changes of variable

$$\rho = r\sin\theta \tag{21}$$

$$z = r\cos\theta \tag{22}$$

$$\lambda = k\sin\xi \tag{23}$$

in eq. (19). We obtain

$$d\tilde{H}_\phi = \frac{k}{8\pi}\,\tilde{I}(r')dr' \int_{C_\xi} \left(\frac{2jk\sin\xi}{\pi r\sin\theta}\right)^{1/2} G(\xi)e^{-jkr\cos(\xi-\theta)}d\xi \tag{24}$$

where

$$G(\xi) = e^{jkr'\cos\theta_0\cos\xi}\left[\cos\theta_0\sin\xi\ J_0(kr'\sin\theta_0\sin\xi)\right. \tag{25}$$

$$\left. -j\sin\theta_0\cos\xi\ J_1(kr'\sin\theta_0\sin\xi)\right]$$

$$+ R(k\cos\xi)e^{-jkr'\cos\theta_0\cos\xi}\left[\cos\theta_0\sin\xi\ J_0(kr'\sin\theta_0\sin\xi)\right.$$

$$\left. + j\sin\theta_0\cos\xi\ J_1(kr'\sin\theta_0\sin\xi)\right]$$

where C_ξ is an appropriate integration contour in the complex ξ-plane.

The complex ξ-plane is shown in Figure 2. The branch cuts between $\xi = -\pi$ and $\xi = 0$, $\xi = \pi$ and $\xi = 2\pi$, ... and the branch cuts on $\Im(\xi) = -\pi/2,\ 3\pi/2,$ ... arise from the factor $(\sin\xi)^{1/2}$ in the integrand of eq. (24). The additional branch cuts, which arise from the reflection coefficient $R(k\sin\xi)$, are defined such that $\Im\sqrt{\hat{\epsilon}_r - \sin^2\xi} = 0$ on the cuts. The exposed sheet is that on which $\Im\sqrt{\hat{\epsilon}_r - \sin^2\xi} < 0$. The reflection coefficient has poles located at

$$\cos\xi = \frac{\pm 1}{\sqrt{\hat{\epsilon}_r + 1}} \tag{26}$$

The poles on the exposed sheet (that is, poles for which $\Im\sqrt{\hat{\epsilon}_r - \sin^2\xi} < 0$) are located where

$$\cos\xi = \frac{-1}{\sqrt{\hat{\epsilon}_r + 1}} \tag{27}$$

The pole which will most strongly influence the field of the conical ring dipole is

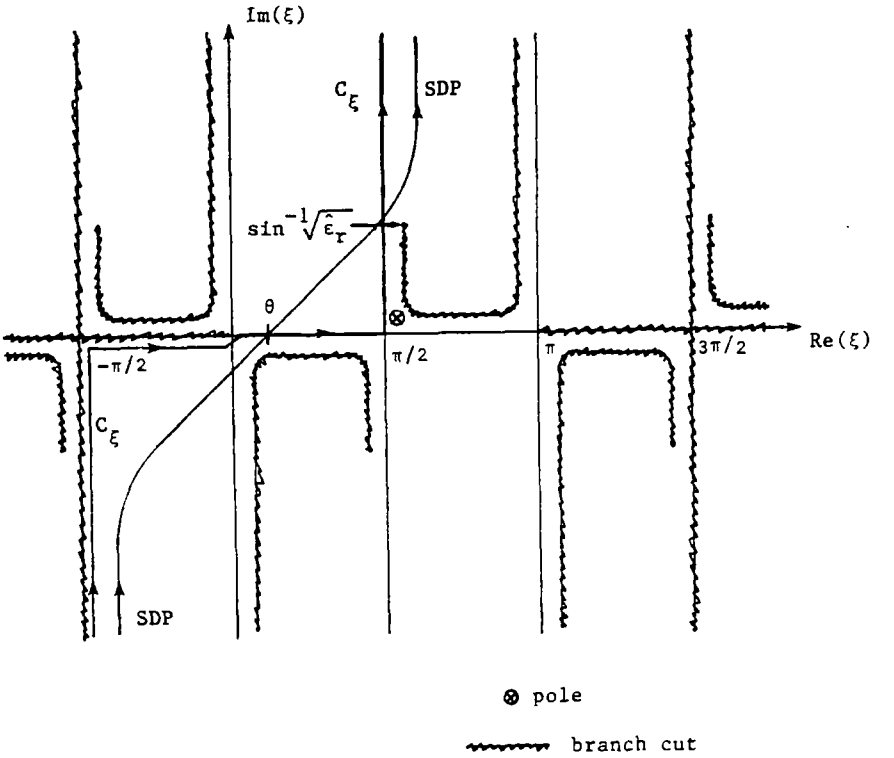

Figure 2: The complex ξ-plane.

located where

$$\xi = \xi_p = \pi/2 + \Delta_r + j\Delta_i \tag{28}$$

where $\Delta_r > 0$ and $\Delta_i > 0$; and Δ_r and Δ_i depend upon $\hat{\epsilon}_r$. This pole is always located between the branch cut originating at $\sin\xi = \sqrt{\hat{\epsilon}_r}$ and the lines $\Re(\xi) = \pi/2$, $\Im(\xi) \geq 0$ and $\Re(\xi) \geq \pi/2$, $\Im(\xi) = 0$. The integration contour C_ξ runs from $\xi = -\pi/2 - j\infty$ to $\xi = -\pi/2$, passing just to the right of the branch cut along $\Im(\xi) = -\pi/2$; thence to $\xi = \pi/2$, passing just beneath the branch cut which originates at $\xi = 0$; and finally to $\xi = \pi/2 + j\infty$.

Now deform the integration contour C_ξ into the steepest-descent path SDP which passes through the point $\xi = \theta$. The steepest-descent path is defined by

the condition

$$\cos(\xi - \theta) = 1 - j\frac{\eta^2}{2} \tag{29}$$

where η is real. Next separate out the singular behavior at $\xi = \xi_p$ of the function $G(\xi)$, writing

$$G(\xi) = \left[G(\xi) - \frac{A}{\xi - \xi_p}\right] + \frac{A}{\xi - \xi_p} \tag{30}$$

where A denotes the residue of $G(\xi)$ at the pole. The sum of the first two terms on the right-hand side of eq. (30) is analytic at $\xi = \xi_p$. We note that in deforming C_ξ into SDP, one may encounter the branch point at $\sin\xi = \sqrt{\hat{\epsilon}_r}$ for observation angles θ greater than some minimum value which depends on $\hat{\epsilon}_r$. It can be shown that the contribution to the total field associated with this branch point and its associated branch cut is small in comparison to the space-wave and ground-wave contributions, and we do not consider it further.

Introduce the approximation

$$\xi = \theta + \eta e^{j\pi/4} \tag{31}$$

near the saddle point. Since $kr >> 1$, we extend the integration range on η to $(-\infty, \infty)$, yielding for the integral in eq. (24)

$$d\tilde{H}_\phi \sim \frac{k\tilde{I}(r')dr'}{8\pi}\left(\frac{2jk}{\pi r}\right)^{1/2} e^{-jkr}e^{j\pi/4}\,. \tag{32}$$

$$\left\{\int_{-\infty}^{\infty} e^{-kr\eta^2/2}\left[G(\theta + \eta e^{j\pi/4}) - \frac{A}{\theta + \eta e^{j\pi/4} - \xi_p}\right] d\eta\right.$$

$$+A\int_{-\infty}^{\infty} e^{-kr\eta^2/2}\frac{d\eta}{\theta+\eta e^{j\pi/4}-\xi_p}\Bigg\}$$

where we have evaluated the slowly varying factor $(\sin\xi)^{1/2}$ at $\xi=\theta$ and extracted it from the integrals. Now the function in square brackets in the first integral of eq. (32) varies slowly with η near the saddle point, so it can be evaluated at $\eta=0$ and extracted from the integral. There remains simply

$$\int_{-\infty}^{\infty} e^{-kr\eta^2/2}d\eta=\left(\frac{2\pi}{kr}\right)^{1/2} \tag{33}$$

The second integral can be evaluated in terms of the error function of complex argument $w(\xi)$, defined by [3]

$$w(\xi)=e^{-\xi^2}\mathrm{erfc}(-j\xi) \tag{34}$$

We have

$$\int_{-\infty}^{\infty}\frac{e^{-kr\eta^2/2}d\eta}{\theta-\xi_p+\eta e^{j\pi/4}}=-j\pi w\left[j\sqrt{\frac{jkr}{2}}(\xi_p-\theta)\right] \tag{35}$$

Expressing $d\tilde{H}_\phi$ in terms of these results and using the relation $d\tilde{E}_\theta=Z_0 d\tilde{H}_\phi$, where $\tilde{E}_\theta$ is the θ-component of the frequency-domain electric field, we obtain

$$d\tilde{E}_\theta = \frac{jkZ_0\tilde{I}(r')dr'}{4\pi r}G(\theta)e^{-jkr} \tag{36}$$

$$\frac{-jk\tilde{I}(r')dr'A}{4\pi r(\theta-\xi_p)}\ e^{-jkr}F_s\left[\sqrt{\frac{jkr}{2}}(\xi_p-\theta)\right]$$

The first term on the right-hand side of eq. (36) represents the space-wave field of the conical ring dipole. The second term represents the ground-wave field. The function $F_s(\cdot)$ is the Sommerfeld attenuation function [4] defined by

$$F_s(\xi) = 1 - \sqrt{\pi}\, \xi w(j\xi) \tag{37}$$

The residue A is easily shown to be

$$A = \left(\frac{2\hat{\epsilon}_r^{3/2}}{\hat{\epsilon}^2 - 1}\right) e^{-jkr' \cos\theta_0 \cos\xi_p} \cdot \tag{38}$$

$$[\sin\xi_p \cos\theta_0 J_0(kr' \sin\theta_0 \sin\xi_p) + j \cos\xi_p \sin\theta_0 J_1(kr' \sin\theta_0 \sin\xi_p)]$$

where

$$\cos\xi_p = \frac{-1}{\sqrt{\hat{\epsilon}_r + 1}} \tag{39}$$

$$\sin\xi_p = \frac{\sqrt{\hat{\epsilon}_r}}{\sqrt{\hat{\epsilon}_r + 1}} \tag{40}$$

This completes the asymptotic analysis of the field of a conical ring dipole over an imperfect ground.

4 The Electromagnetic Field of VPD-II

In this section we use the result given in eq. (36) for the field of the conical ring dipole to evaluate the field of VPD-II. We consider first the space-wave field.

4.1 Space-Wave Field

The space-wave electric field $d\tilde{E}_{\theta s}$ of the conical ring dipole is given for $kr >> 1$ by

$$d\tilde{E}_{\theta s} = \frac{jkZ_0\tilde{I}_0(j\omega)}{4\pi r}e^{-jkr}\left(1-\frac{r'}{r_0}\right)e^{-jkr'}G(r';\theta)dr' \tag{41}$$

where $r'/r_0 < 1$ and we have indicated the dependence of G upon r'. To obtain the space-wave field for VPD-II, we simply integrate the expression given in eq. (41) over r' from $r' = 0$ to $r' = r_0$. We express the Bessel functions which appear in $G(r';\theta)$ in terms of their integral representations as follows:

$$J_0(kr'\sin\theta_0\sin\theta) = \frac{1}{2\pi}\int_0^{2\pi} e^{jkr'\sin\theta_0\sin\theta\cos\phi'}d\phi' \tag{42}$$

$$J_1(kr'\sin\theta_0\sin\theta) = \frac{-j}{2\pi}\int_0^{2\pi} e^{jkr'\sin\theta_0\sin\theta\cos\phi'}\cos\phi' d\phi' \tag{43}$$

We next carry out the integrations over r'. We obtain for the space-wave electric field $\tilde{E}_{\theta s}$ the integral expression

$$\begin{aligned}\tilde{E}_{\theta s}(r,\theta) &= \frac{-Z_0\tilde{I}_0(j\omega)e^{-jkr}}{4\pi r}\frac{1}{2\pi}\int_0^{2\pi} d\phi' \cdot \\ &\left\{\left(\frac{-\sin\theta\cos\theta_0+\cos\theta\sin\theta_0\cos\phi'}{1-\cos\theta\cos\theta_0-\sin\theta\sin\theta_0\cos\phi'}\right)\cdot\right. \\ &\left.\left[1-\frac{1-e^{-jkr_0(1-\cos\theta\cos\theta_0-\sin\theta\sin\theta_0\cos\phi')}}{jkr_0(1-\cos\theta\cos\theta_0-\sin\theta\sin\theta_0\cos\phi')}\right]-\right.\end{aligned} \tag{44}$$

$$R(k\cos\theta)\left(\frac{\sin\theta\cos\theta_0+\cos\theta\sin\theta_0\cos\phi'}{1+\cos\theta\cos\theta_0-\sin\theta\sin\theta_0\cos\phi'}\right)\cdot$$

$$\left[1-\frac{1-e^{jkr_0(1+\cos\theta\cos\theta_0-\sin\theta\sin\theta_0\cos\phi')}}{jkr_0(1+\cos\theta\cos\theta_0-\sin\theta\sin\theta_0\cos\phi')}\right]\Bigg\}$$

which agrees with the integral representation for the space-wave field given in [1]. Evaluation of the integral over ϕ' and of the space-wave field was discussed in [1].

4.2 Ground-Wave Field

The ground-wave electric field $d\tilde{E}_{\theta g}$ of the conical ring dipole is given for $kr >> 1$ by

$$d\tilde{E}_{\theta g} = \frac{-jkZ_0\tilde{I}_0(j\omega)e^{-jkr}}{4\pi r(\theta-\xi_p)}\ F_s\left[\sqrt{\frac{jkr}{2}}(\xi_p-\theta)\right]\cdot \tag{45}$$

$$\left(1-\frac{r'}{r_0}\right)e^{-jkr'}A(r')dr'$$

where $r'/r_0 < 1$ and where we have indicated the dependence of A upon r'. To obtain the ground-wave field of VPD-II, we integrate the expression given in eq. (45) over r' from $r'=0$ to $r'=r_0$. Again expressing the Bessel functions in terms of their integral representations and carrying out the integration over r', we obtain for the ground-wave electric field $\tilde{E}_{\theta g}$

$$\tilde{E}_{\theta g}(r,\theta) = \frac{-Z_0\tilde{I}_0(j\omega)e^{-jkr}}{4\pi r(\theta-\xi_p)}\left(\frac{2\hat{\epsilon}_r^{3/2}}{\hat{\epsilon}_r^2-1}\right)F_s\left[\sqrt{\frac{jkr}{2}}(\xi_p-\theta)\right]\cdot \tag{46}$$

$$\frac{1}{2\pi}\int_0^{2\pi} d\phi' \left(\frac{\sin\xi_p\cos\theta_0+\cos\xi_p\sin\theta_0\cos\phi'}{1+\cos\xi_p\cos\theta_0-\sin\xi_0\sin\theta_0\cos\phi'}\right)\cdot$$

$$\left[1-\frac{1-e^{-jkr_0(1+\cos\theta_0\cos\xi_p-\sin\xi_p\sin\theta_0\cos\phi')}}{jkr_0(1+\cos\xi_p\cos\theta_0-\sin\xi_p\sin\theta_0\cos\phi')}\right]$$

This expression can be written in the form

$$\tilde{E}_{\theta g}(r,\theta) = \frac{-Z_0\tilde{I}_0(j\omega)e^{-jkr}}{4\pi r(\theta-\xi_p)}\left(\frac{2\hat{\epsilon}_r^{3/2}}{\hat{\epsilon}_r^2-1}\right)F\left[\sqrt{\frac{jkr}{2}}(\xi_p-\theta)\right]\cdot \tag{47}$$

$$\left(\hat{I}_1-\frac{\hat{I}_2}{jkr_0}+\frac{\hat{I}_3}{jkr_0}e^{-jkr_0}\right)$$

where

$$\hat{I}_1=\frac{1}{2\pi}\int_0^{2\pi} d\phi'\left(\frac{\sin\xi_0\cos\theta_0+\cos\xi_p\sin\theta_0\cos\phi'}{1+\cos\xi_p\cos\theta_0-\sin\xi_p\sin\theta_0\cos\phi'}\right) \tag{48}$$

$$\hat{I}_2=\frac{1}{2\pi}\int_0^{2\pi} d\phi'\frac{(\sin\xi_p\cos\theta_0+\cos\xi_p\sin\theta_0\cos\phi')}{(1+\cos\xi_p\cos\theta_0-\sin\xi_p\sin\theta_0\cos\phi')^2} \tag{49}$$

$$\hat{I}_3=\frac{1}{2\pi}\int_0^{2\pi} d\phi' \quad \frac{(\sin\xi_p\cos\theta_0+\cos\xi_p\sin\theta_0\cos\phi')}{(1+\cos\xi_p\cos\theta_0-\sin\xi_p\sin\theta_0\cos\phi')^2}\cdot \tag{50}$$

$$e^{-jkr_0(\cos\theta_0\cos\xi_p-\sin\xi_p\sin\theta_0\cos\phi')}$$

The integrals $\hat{I}_1$ and $\hat{I}_2$ can be evaluated in closed form through the use of the residue theorem. The results are

$$\hat{I}_1=\csc\xi_p-\cot\xi_p=\frac{1}{\sqrt{\hat{\epsilon}_r}}\left(\sqrt{\hat{\epsilon}_r+1}+1\right) \tag{51}$$

$$\hat{I}_2 = \frac{\sin\xi_p}{(\cos\xi_p + \cos\theta_0)^2} = \frac{\sqrt{\hat{\epsilon}_r(\hat{\epsilon}_r + 1)}}{(\sqrt{\epsilon_r + 1}\cos\theta_0 - 1)^2} \tag{52}$$

The integral $\hat{I}_3$ cannot be evaluated in closed form. It can be evaluated numerically if kr_0 is not too large; and if $kr >> 1$, asymptotic methods are appropriate. Using the methods described in [1], we can show that when $kr_0 >> 1$,

$$\hat{I}_3 \sim \frac{1}{\sqrt{2\pi j k r_0 \sin\xi_0 \sin\theta_0}} \left\{ \frac{j\sin(\xi_p - \theta_0) e^{-jkr_0\cos(\xi_p - \theta_0)}}{[1 + \cos(\xi_p - \theta_0)]^2} \right. \tag{53}$$

$$\left. + \frac{\sin(\xi_p + \theta_0) e^{-jkr_0\cos(\xi_p + \theta_0)}}{[1 + \cos(\xi_p + \theta_0)]^2} \right\}$$

The frequency-domain analysis of the electromagnetic field radiated by the VPD-II antenna is now complete. We next consider representative numerical results for the field in the time domain.

5 Representative Numerical Results

We use the equivalent circuit shown in Figure 3 and discussed in [1] to obtain the frequency-domain current at the antenna feed $\tilde{I}_0(j\omega)$. We have

$$\tilde{I}_0(j\omega) = \frac{j\omega\tau_m C_a V_0}{1 + j\omega\{\tau_a + \tau_m(1 + C_a/C_m) + j\omega[\tau_a\tau_m + (1 + j\omega\tau_m)/\omega_a^2]\}} \tag{54}$$

where V_0 is the pulser charge voltage and

$$\tau_a = R_a C_a \tag{55}$$

$$\tau_m = R_m C_m \tag{56}$$

$$\omega_a^2 = \frac{1}{L_m C_a} \tag{57}$$

with

R_a = antenna input resistance = 60 Ω

C_a = antenna capacitance = 2.9 nF

R_m = Marx generator resistance = 3.7 kΩ

C_m = Marx capacitance = 5.4 nF

L_m = Marx inductance = 0.245 μH

The relative permittivity of the ground is described by [5]

$$\hat{\epsilon}_r = \left(\sqrt{\epsilon_{r\infty}} + \sqrt{\frac{\sigma_0}{j\omega\epsilon_0}} \right)^2 \tag{58}$$

where $\epsilon_{r\infty}$ is the high-frequency relative permittivity of the ground and σ_0 is the low-frequency conductivity. We used values of $\epsilon_{r\infty} = 8$ and $\sigma_0 = 3 \times 10^{-3}$ S m^{-1} to represent the ground near VPD-II.

Using numerical inverse Fourier transformation of the relevant expressions for the frequency-domain electric field, we have calculated the normalized electric field $e_\theta(r, \theta; t)$ defined by

$$e_\theta(r, \theta; t) = \frac{r E_\theta(r, \theta; t - r/c)}{V_0} \tag{59}$$

where

$$E_\theta = E_{\theta s} + E_{\theta g} \tag{60}$$

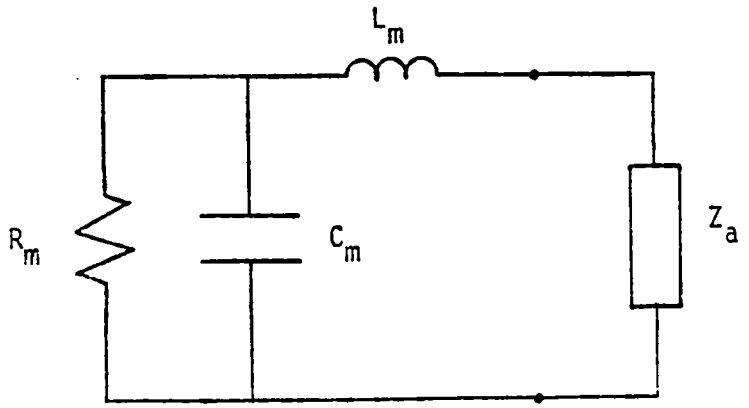

Figure 3: Equivalent circuit for the Marx generator and antenna.

We remark that e_θ is independent of r when only the space-wave field is considered; this is not the case when the ground wave is included. Accordingly, we present results for $e_\theta(r, \theta; t)$ at various ranges r and angles θ.

Plots of $e_\theta(r, \theta' t)$ as a function of time t for fixed values of r and three values of θ are shown in Figures 4 – 7. For each value of r, the peak value and the rise rate of r_θ decrease as θ is increased. We note, however, that e_θ does not vanish at $\theta = 90°$; the space-wave contribution to e_θ vanishes at this angle, but the ground-wave contribution does not.

Comparisons among curves for the same angle but different ranges make it evident that at $\theta = 80°$, the normalized radiated field is not very sensitive to the range r. This result indicates that the space wave is strongly dominant at this observation angle. At $\theta = 90°$, the space wave is absent and the resulting stronger

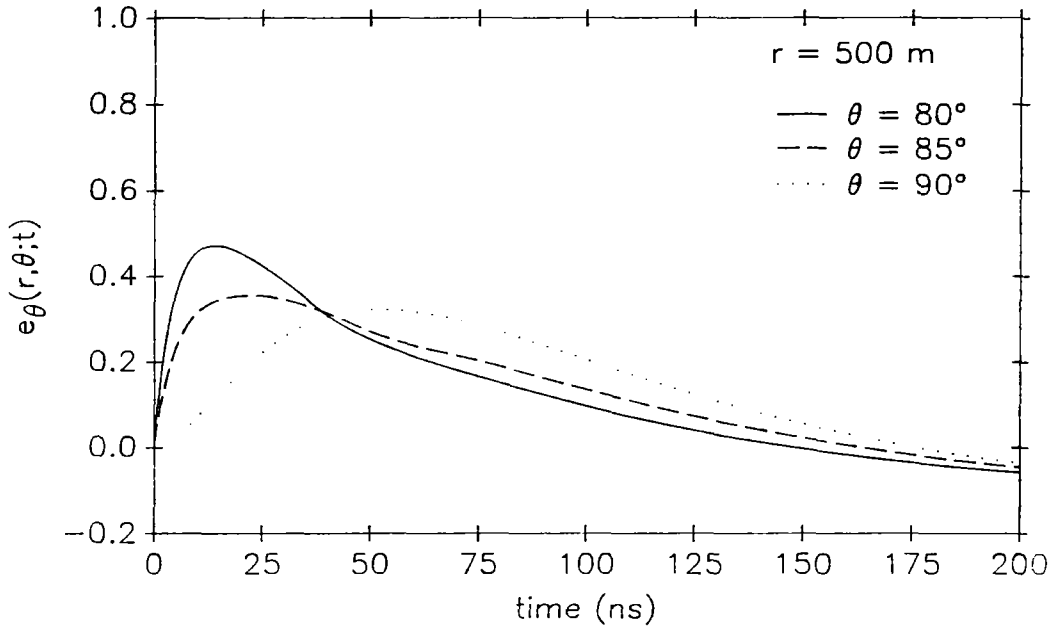

Figure 4: Normalized electric field $e_\theta(r, \theta; t)$ vs. t : $r = 500$ m; $\theta = 80°$, $85°$, $90°$.

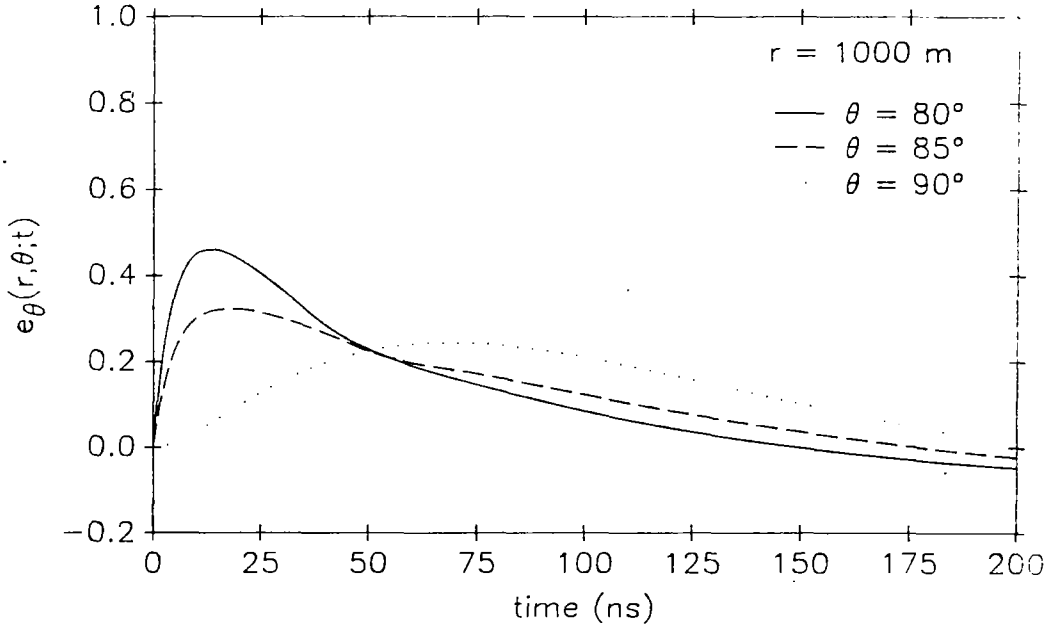

Figure 5: Normalized electric field $e_\theta(r, \theta; t)$ vs. t : $r = 1000$ m; $\theta = 80°$, $85°$, $90°$.

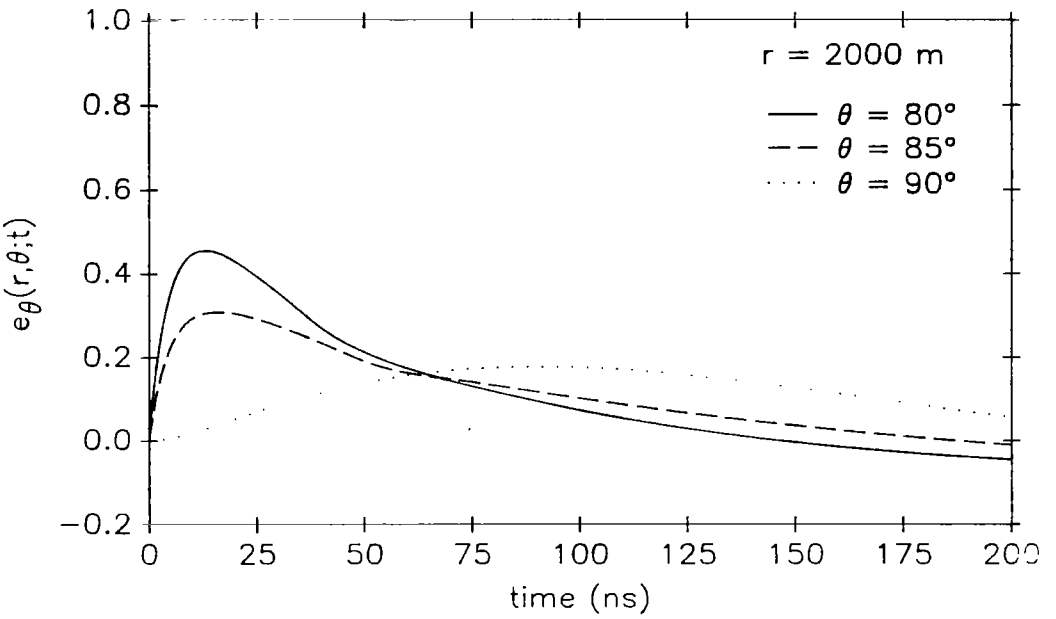

Figure 6: Normalized electric field $e_\theta(r, \theta; t)$ vs. t : $r = 2000$ m; $\theta = 80°, 85°, 90°$.

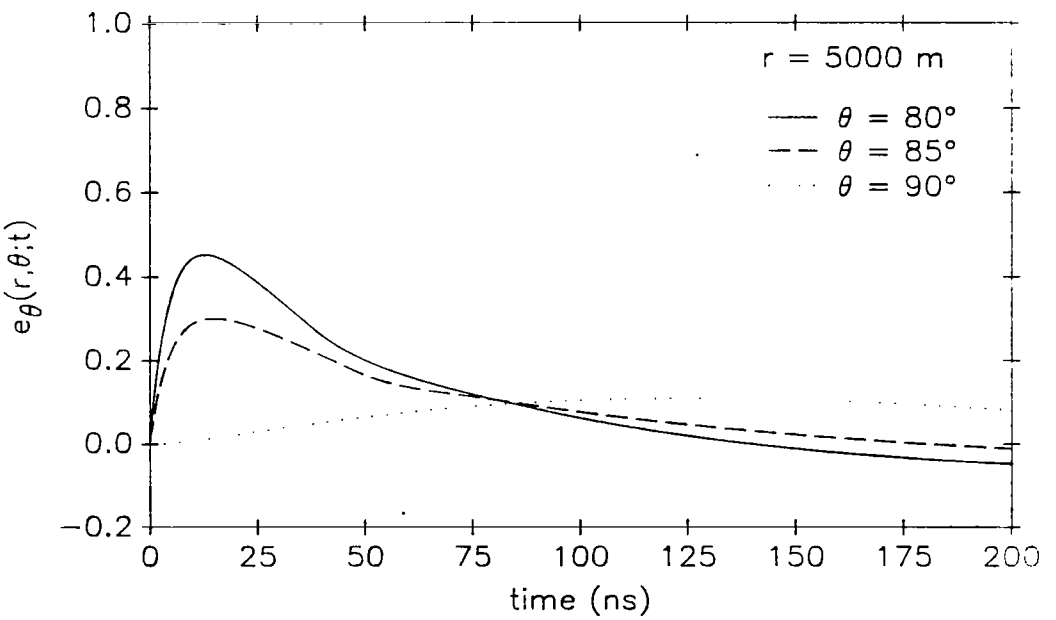

Figure 7: Normalized electric field $e_\theta(r, \theta; t)$ vs. t : $r = 5000$ m; $\theta = 80°, 85°, 90°$.

dependence on range is evident.

The electric field strength seen by an observer near the air-ground interface is readily calculated from the plots. Assuming $V_0 = 3.5$ MV, we find that at $\theta = 90°$:

$$E_{\theta,pk} \cong 2.27 \text{ kV/m at } r = 500 \text{ m}$$
$$845 \text{ V/m at } r = 1 \text{ km}$$
$$314 \text{ V/m at } r = 2 \text{ km}$$
$$77 \text{ V/m at } r = 5 \text{ km}$$

The ground-wave field strength decreases approximately as $r^{-3/2}$. Furthermore, because of the dispersion associated with the propagation of the ground wave, the rise rate decreases with increasing range.

6 Concluding Remarks

We have modeled the antenna of the VPD-II EMP environment simulator as a distribution of "conical ring" dipoles over an imperfect ground. The field of a single such dipole is evaluated in the frequency domain using saddle-point integration techniques to yield an asymptotic representation for the field valid when $kr \to \infty$. The space-wave and ground-wave contributions to the total field arise from this asymptotic representation. Then by integrating these field contributions over the distribution of conical ring dipoles, using the surface current density established on the VPD-II antenna by the nonuniform resistive loading, we obtained the frequency-domain radiated field. Equivalent circuits for the Marx generator

and the antenna were used to obtain the current at the feed point of the antenna. The time-domain field was evaluated via numerical inverse Fourier transformation of the frequency-domain representations.

We have presented numerical results illustrating the behavior of the radiated field as a function of time at various observation angles and ranges. For observation angles less than approximately 80°, the space-wave field is dominant. This field decays as r^{-1}. The ground-wave field becomes increasingly important as the observation angle approaches 90°. At $\theta = 90°$, the space wave vanishes and the ground wave, which decays approximately as $r^{-3/2}$, is the only component of the field. At a ground range of one kilometer, the peak value of the electric field in the air-ground interface is less than one kilovolt per meter.

References

[1] Kendall F. Casey, "The External Environment of VPD-II: The Space-Wave Field", *Sensor and Simulation Notes*, Note 323, April 1990.

[2] R. F. Harrington, *Time-Harmonic Electromagnetic Fields*, McGraw-Hill, New York, 1961, pp. 100, 135.

[3] M. Abramowitz and I. A. Stegun, eds., *Handbook of Mathematical Functions*, AMS-55, National Bureau of Standards, p. 297.

[4] J. R. Wait, "Characteristics of Antennas over Lossy Earth", in *Antenna Theory* (R. E. Collin and F. J. Zucker, eds.) McGraw-Hill, New York, 1969, Part II, p. 391.

[5] M. A. Messier, "The Propagation of an Electromagnetic Impulse through Soil: Influence of Frequency-Dependent Parameters", Mission Research Corporation Report No. MRC-N-415, 1980.